

# Microscopic quark study of the $\eta$ and $\eta'$ masses

O. Lakhina\*

Center for Nuclear Research, Department of Physics, Kent State University, Kent OH 44242, USA

P. Bicudo†

CFTP, Dep. Física, Instituto Superior Técnico, Av. Rovisco Pais, 1049-001 Lisboa, Portugal.

We show that it is necessary to go beyond the BCS (rainbow-ladder) approximation to split the  $\eta$  and  $\eta'$  masses from the  $\pi$  and  $K$  masses. We determine the self-consistent set of one-quark-loop diagrams both for the Schwinger-Dyson quark mass gap equation and for the Bethe-Salpeter quark-antiquark boundstate equation. We identify the dominant diagrams, and we focus on the boundstate equation. We detail the Bethe-Salpeter equation, adding the dominant new diagram to the BCS kernel. The relevant numerical techniques are also discussed. The ideal cases of one, two and three light flavors, relevant to lattice QCD are also explored, together with the case of realistic current quark masses.

## I. INTRODUCTION

Many years ago Weinberg [1] noticed the difficulty to account for the  $\eta$  -  $\eta'$  mass difference. He baptized this difficulty as the U(1) problem. Here we address the U(1) problem in the microscopic perspective of quark models. Notice that all effective models of QCD faced this problem. In their second paper, Nambu and Jona-Lasinio [2] include the isospin-dependent pseudoscalar contact interactions in their model to account for the  $\eta$  -  $\eta'$  mass difference, which are reminiscent of scalar and pseudoscalar meson exchanges. In this sense it is similar to the original  $\sigma$  model of Gell-Mann and Lévy [3], where the pseudoscalar exchange does not include the isosinglet. A different determinant interaction was invented by 't Hooft [4] to split the  $\eta$  and  $\eta'$  masses. With three flavors this

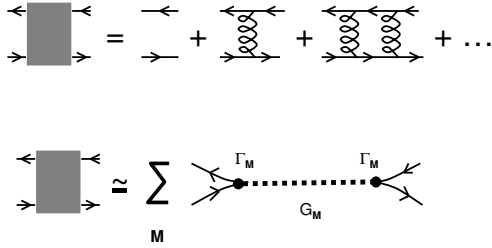


FIG. 1: We show the ladder, minimal geometric series of diagrams to include the mesons as Bethe-Salpeter quark-antiquark bound states. This ladder is isopin invariant, i.e. in the chiral limit the spectrum is identical for the  $\pi$ , the  $K$ , the  $\eta$  and the  $\eta'$ . Notice that, starting in this figure, for simplicity we depict in the same way the bare and dressed gluon-quark-quark vertices.

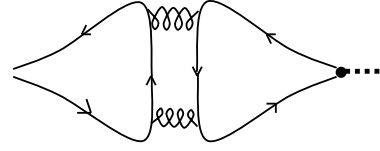


FIG. 2: We show the minimal figure necessary to split the  $\eta$  mass from the  $\eta'$  mass. This diagram, or any other diagram where the *in* fermion lines are not continued to the *out* fermion lines, only contributes to  $I = 0$  mesons. For other mesons it cancels.

is a tree-body interaction. Recently a four-body interaction was further added by Osipov, Hiller and Providência [5] to stabilize the vacuum. At a more fundamental level is Lattice QCD, where both the quark and gluon fields are considered. However the Lattice QCD simulations only reproduce the  $\eta$  -  $\eta'$  experimental mass difference with the indirect technique [6, 7] of the hairpin diagram [8], or with the extrapolation of the current quark mass [9]. we aim to understand how the  $\eta$  -  $\eta'$  mass difference arises in a microscopic Quark Model.

In the Quark Model, and in other related frameworks such as the Schwinger-Dyson equations, the minimal computations of the meson masses are performed in the *ladder* approximation. The ladder geometric series is depicted in Fig. 1. In this case the kernel (the set of diagrams that is iterated in the Bethe-Salpeter equation) is a one-gluon exchange, or an effective quark-antiquark interaction resulting from the integration of the gluon field. In the limit of equal quark masses, the ladder approximation does not separate the  $\eta$  from the  $\eta'$ . Notice that any consistent quark model should also include consistently chiral symmetry breaking. Then, in the mass gap equation, the ladder approximation is equivalent to the *rainbow*, or *BCS* approximation. In the BCS approximation, the chiral symmetry is not a  $SU(N_f)$  symmetry (where  $N_f$  is the number of light fermions), but a  $U(N_f)$

\*Electronic address: olakhina@kent.edu

†Electronic address: bicudo@ist.utl.pt

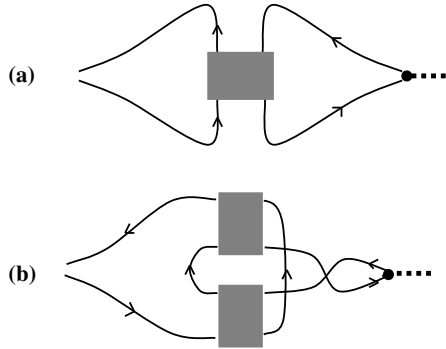


FIG. 3: In non-perturbative QCD, the minimal diagram should be dressed with all possible gluon exchange insertions. We show in (a) the minimal one-ladder-figure necessary to split the  $\eta$  mass from the  $\eta'$  mass. In (b) we show a two-ladder diagram, equivalent to the coupling to the initial one-meson channel to the two-meson channels. Both these diagrams only contribute to  $I = 0$  mesons.

global symmetry.

To address the  $\eta - \eta'$  mass difference problem one has to go beyond the BCS approximation [10, 11]. It is necessary to add at least one quark loop in the mass gap equation, including quark-antiquark annihilation and creation in the quark-antiquark boundstate equation. The minimal extension to the kernel of the boundstate equation is shown in Fig. 2. Notice that this diagram includes two  $AVV$  triangles, and thus includes the Adler-Bell-Jackiw anomaly [12, 13, 14], in this case the non-abelian anomaly, also related to the  $U(1)$  problem [15]. The anomaly is an ultraviolet effect and it is a relevant effect. For instance for  $\eta$ , the anomalous electromagnetic decay to  $\gamma\gamma$  is of the same order as the hadronic decays.

There has been an attempt to compute the diagram of Fig. 1 in SDE approach and explore its effect on  $\eta - \eta'$  mass difference [16]. However, certain assumptions were made about the infrared behavior of the gluon propagator, which have been shown later not to be true [17].

Moreover, in non-perturbative infrared QCD, the diagram of Fig. 2 is not really complete. The kernel should include all diagrams of the same class [10]. In particular the  $\eta - \eta'$  mass difference is a non-perturbative problem and there is no reason to include only two gluons, or two effective quark-antiquark interactions. Inasmuch as the full geometric series included in the boundstate minimal boundstate study, the diagram of Fig. 2 should be dressed with at least a full ladder series. In Fig. 3 (a) we include all the possible number of gluon exchanges, and this is equivalent to include a full meson-like ladder. This diagram includes all possible t-channel exchanges of mesons.

A different possible way to dress the diagram is depicted in Fig. 3 (b). In this case the diagrams are resummed in two ladders. This is equivalent to couple the

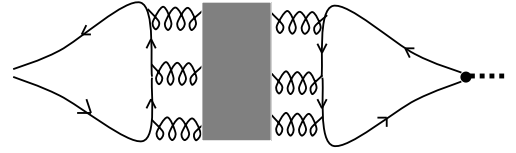


FIG. 4: It is also possible to dress the minimal diagram with a pure-gluon ladder. We show a different dressing, equivalent to couple the pseudoscalar mesons to glueballs. Notice that with transverse gluons at least three gluons are needed to constitute a pseudoscalar  $J^{PC} = 0^{-+}$  glueball. This diagram also contributes to  $I = 0$  mesons, but it is suppressed by the large three-gluon glueball masses.

original one meson to all possible two-meson channels. Notice that, since a pseudoscalar cannot couple to two pseudoscalars, the lightest coupled channel includes one pseudoscalar and one vector, or one pseudoscalar and one scalar. So this channel is already quite heavier than the original one meson channel of Fig. 3 (a). In Fig. 4 we exchange all the possible number of gluons, not between the quark lines, but between the gluon lines, include a full glueball-like ladder. This diagram is equivalent to couple the pseudoscalar mesons to glueballs. Notice that with transverse gluons at least three gluons are needed to constitute a pseudoscalar  $J^{PC} = 0^{-+}$  glueball. Both in lattice QCD and in constituent quark models, including models where the gluon mass is generated with a mass gap or Schwinger-Dyson equation, the three gluon glueballs are quite heavy, much heavier than the mesonic coupled channel of one pseudoscalar and one vector. Thus we estimate that the leading non-perturbative diagram contributing to the  $\eta - \eta'$  mass difference is the t-channel one meson exchange represented in Fig. 3 (a). In particular, because the pion is a light meson, the exchange of a virtual pion should be relevant. This is consistent with the results of the Nambu and Jona-Lasinio model and of the  $\sigma$  model.

Importantly, chiral symmetry forces us to use a self-consistent set of diagrams. Similarly to the sets of diagrams that preserve gauge invariance when a photon is coupled, in the study of pseudoscalar mesons a self-consistent set of diagrams is necessary.

Notice that different frameworks may be used to compute the necessary diagrams. We may address the  $U(1)$  problem in the equal-time quark model formalism, or we may use the related euclidian-time Schwinger-Dyson formalism. Although the quark model is explicitly confining, and able to reproduce the hadronic spectra up to high excitations, the separation of the quark and antiquark propagators [10] would force us to use a much too large number of diagrams. Thus we will work in the Schwinger-Dyson formalism, with Euclidian momenta integrations, expecting that our results will also apply to the quark model.

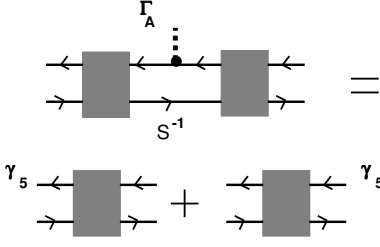


FIG. 5: We show the ladder Ward Identity, crucial to verify that the Schwinger Dyson mass gap equation is consistent with the Bethe Salpeter bound state equation.

In Section II we determine the necessary self-consistent set of diagrams both for the Schwinger-Dyson quark mass gap equation and for the Bethe-Salpeter quark-antiquark boundstate equation. Because the full set of diagrams goes beyond the present state of the art techniques, in Section III we identify the dominant diagrams. Notice that the effect of meson exchange in the mass gap equation has already been estimated, and thus we focus here on the boundstate equation only. We also detail the Bethe Salpeter equation, adding the dominant new  $U(1)$  splitting diagram to the BCS kernel. In Section IV we discuss the relevant numerical techniques and we show the results for the  $\eta$  and  $\eta'$  masses. The ideal case of two light flavors, relevant to lattice QCD is also explored, together with the case of realistic current quark masses with three flavors. In section V we conclude.

## II. A CHIRALLY SELF-CONSISTENT CLASS OF DIAGRAMS

We choose the Schwinger-Dyson equation (SDE) formalism to investigate the effect of the diagrams that contribute differently to the masses of isoscalars ( $\eta$  or  $\eta'$ ) and isovector ( $\pi^0$ ). For recent reviews on the SDEs and their use in hadron physics, see for example [18, 19].

The SDEs are an infinite number of coupled integral equations; a simultaneous, self-consistent solution of the complete set is equivalent to a solution of the theory. In practice, the complete solution of SDEs is not possible for QCD. Therefore one employs a truncation scheme by solving only the equations important to the problem under consideration and making assumptions for the solutions of the other equations.

The simplest Schwinger-Dyson equation is the gap equation for the quark propagator. It provides the relationship between the quark propagator, the gluon propagator and the quark-gluon vertex. The exact form of this equation is,

$$S(p)^{-1} = Z_2 (i\gamma \cdot p + m_{bm}) + Z_1 \int \frac{d^4 q}{(2\pi)^4} g^2 D_{\mu\nu}(q) \frac{\lambda^a}{2} \gamma_\mu S(p+q) \Gamma_\nu^a(q, p), \quad (1)$$

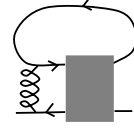


FIG. 6: Contribution of the meson exchange kernel to the mass gap Schwinger-Dyson equation

where  $S(p)$  is the flavor dependent fully dressed quark propagator, which has the form:

$$S(p) = \frac{1}{i \not{p} A(p^2) + B(p^2)}, \quad (2)$$

$D_{\mu\nu}(p-q)$  is the gluon propagator, and  $\Gamma_\nu^a(q, p)$  is the quark-gluon vertex,  $a$  denotes the flavor of the quark. The propagators and the vertex in this equation are dressed and renormalized.  $Z_1$  and  $Z_2$  are the renormalization constants of the quark-gluon vertex and the quark wave function, and  $m_{bm}$  is the bare quark mass.

The Bethe-Salpeter equation is used to study two-particle bound states (mesons). By solving the Bethe-Salpeter equation one obtains the Bethe-Salpeter amplitude which, after proper normalization, completely describes the meson as the bound state of a quark and an antiquark. The Bethe-Salpeter amplitude corresponds to the amputated one-particle-irreducible quark-meson vertex, and its Lorentz structure depends on the quantum numbers of the meson of interest. The exact Bethe-Salpeter equation for the meson can be written as,

$$\Gamma_M(p_1, p_2) = \int \frac{d^4 q}{(2\pi)^4} K(q) S(p_1 + q) \Gamma_M(p_1 + q, p_2 + q) S(p_2 + q), \quad (3)$$

where  $\Gamma_M(p; P)$  is the Bethe-Salpeter amplitude for the meson  $M$ . The Bethe-Salpeter amplitude depends on the quark momenta  $p_1$  and  $p_2$ . If  $m$  is the bound state mass then equation (3) is only valid for  $P^2 = (p_1 - p_2)^2 = -m^2$ , where  $P$  is the total momentum of the meson. The kernel  $K(q)$  is the irreducible quark-antiquark scattering kernel.

The truncated mass gap SDE and the BSE have to be consistent with each other to preserve the chiral symmetry of QCD. This self-consistency is crucial for the pion to be a massless boundstate in the chiral limit. It has been shown that if one inserts the Bethe Salpeter vertex  $\Gamma$  in all possible dressed quark propagators  $S(p)$  present in the SDE for the quark self-energy, one must recover the kernel of the BSE. Inversely, if one removes the Bethe-Salpeter vertex from the BSE, replacing  $S\Gamma S$  by the propagator  $S$ , one must recover the self-energy of the SDE. This chiral self-consistent relation has already been applied to self-energies and to Bethe Salpeter kernels containing the infinite ladder series of diagrams [10, 20, 21].

Let us first show that using the rainbow-ladder truncation (BCS approximation) one obtains a self-consistent

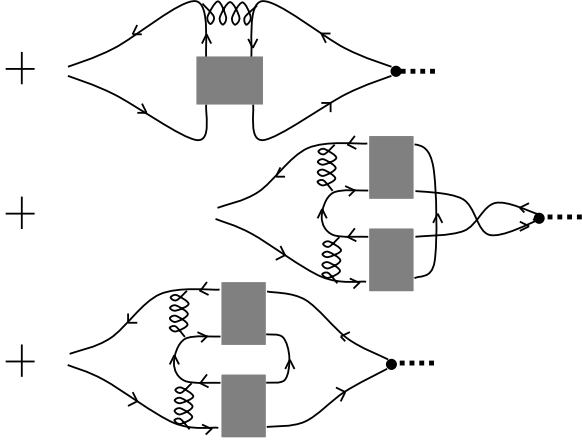


FIG. 7: Contribution of the meson exchange kernel to the boundstate Bethe-Salpeter equation

set of equations for quark propagator, bound states and vertices. After that, an analogous set of equations will be derived for a different truncation, which includes the diagrams necessary for generating  $\eta$ - $\eta'$  mass.

The rainbow truncation of Schwinger-Dyson equation for the quark propagator includes the replacement of the dressed quark-gluon vertex by the bare one,

$$Z_1 g^2 D_{\mu\nu}(q) \Gamma_\nu^a(q, p) \rightarrow \frac{G(q^2)}{q^2} T_{\mu\nu}(q) \frac{\lambda^a}{2} \gamma_\nu, \quad (4)$$

where  $G(q^2)$  is the effective running coupling,  $q$  is the gluon momentum, and  $T_{\mu\nu}(q) = \delta_{\mu\nu} - q_\mu q_\nu / q^2$  is the transverse operator in Landau gauge. The quantity  $T_{\mu\nu}(q)/q^2$  is the free gluon propagator.

In the rainbow truncation the equation (1) becomes,

$$S(p)^{-1} = S_0^{-1}(p) + \frac{4}{3} \int \frac{d^4 q}{(2\pi)^4} \frac{T_{\mu\nu}(q)}{q^2} G(q^2) \gamma_\mu S(p+q) \gamma_\nu, \quad (5)$$

where  $S_0(p) = (i \not{p} + m)^{-1}$  is the bare quark propagator,  $m$  is the current quark mass.

The equation (5) increases the gap between the quark and antiquark dispersion relations (which is almost zero for bare propagators) and generates the dynamical mass  $M = \sqrt{B^2(p^2)/A^2(p^2)}$ . Because of the color structure of the eqn. (5), the tadpole does not contribute. Multiplying both sides of eqn. (5) with  $\gamma_5$  and summing leads to,

$$S(p_1)^{-1} \gamma_5 + \gamma_5 S(p_2)^{-1} = S_0(p_1)^{-1} \gamma_5 + \gamma_5 S_0(p_2)^{-1} - \int \frac{d^4 q}{(2\pi)^4} \frac{T_{\mu\nu}(q)}{q^2} G(q^2) \gamma_\mu [S(p_1 + q) \gamma_5 + \gamma_5 S(p_2 + q)] \gamma_\nu,$$

which is the Bethe Salpeter equation for the vertex,

$$\Gamma_A(p_1, p_2) = \gamma_A(p_1, p_2) + \int \frac{d^4 q}{(2\pi)^4} K(q) S(p_1 + q) \Gamma_A(p_1 + q, p_2 + q) S(p_2 + q), \quad (6)$$

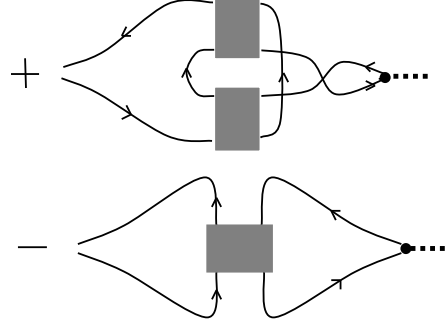


FIG. 8: Non-perturbative part of the kernel contributing only to flavor singlet  $\eta'$  mass.

if the bare  $\gamma_A$  and dressed  $\Gamma_A$  vertices are respectively defined with the same Axial Ward Identity for an isovector,

$$\Gamma_A(p_1, p_2) = S^{-1}(p_1) \gamma_5 + \gamma_5 S^{-1}(p_2), \quad (7)$$

$$\gamma_A(p_1, p_2) = S_0^{-1}(p_1) \gamma_5 + \gamma_5 S_0^{-1}(p_2), \quad (8)$$

and the kernel of the BSE is approximated by the one-gluon exchange (ladder truncation, or BCS approximation),

$$K(q) \rightarrow -\frac{G(q^2)}{q^2} T_{\mu\nu}(q) \frac{\lambda^c}{2} \gamma_\mu \otimes \frac{\lambda^c}{2} \gamma_\nu. \quad (9)$$

The fact that Axial Ward identity is consistent with the ladder approximation for the bound state and the rainbow approximation for the quark self energy equation ensures that this truncation respects the chiral symmetry of QCD. Both approximations are equivalent to the planar diagram expansion which is characteristic of the Quark Model.

The bare vertex  $\gamma_A$  can be computed from the bare quark propagator using (8),

$$\gamma_A(P) = (i \not{P} + 2m) \gamma_5, \quad P = p_1 - p_2, \quad (10)$$

where  $m$  is the current quark mass.  $\gamma_A$  is the particular part of the Bethe Salpeter equation for the vertex (6), and it vanishes when the current quark mass  $m$  is small (chiral limit) and at the same time the total momentum  $P^\mu$  of the vertex is small.

At this point it is important to clarify that in general, as it follows from (10), the bare vertex  $\gamma_A$  is a combination of the axial vector vertex  $\gamma^\mu \gamma_5$  and the pseudoscalar vertex  $\gamma_5$ . In the chiral limit  $\gamma_A$  becomes pure axial vector vertex contracted with momentum, and in the limit of vanishing momentum  $P_\mu$  it becomes pure pseudoscalar vertex multiplied by the current quark mass. For simplicity (and because they are defined with the Axial Ward identity (7) and (8)), in the rest of this paper  $\gamma_A$  will be called the bare axial vertex and  $\Gamma_A$  will be called the dressed axial vertex, although they possess a more general Dirac structure.

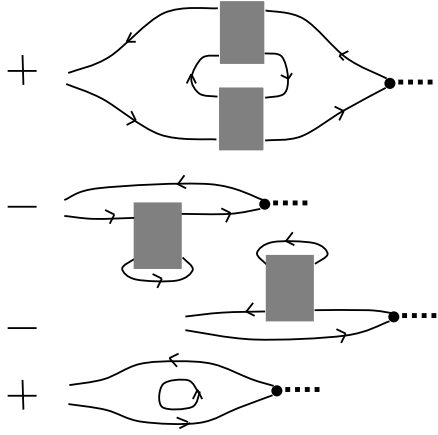


FIG. 9: Non-perturbative part of the kernel shifting all the pseudoscalar masses equally.

The dressed vertex  $\Gamma_A$  can be computed from the dressed quark propagator (2) using (7),

$$\Gamma_A(p_1, p_2) = [iA(p_1)\not{p}_1 - iA(p_2)\not{p}_2 + B(p_1) + B(p_2)]\gamma_5. \quad (11)$$

$\Gamma_A$  is finite providing spontaneous chiral symmetry breaking occurs in eqn. (5) and a dynamical mass of the quark is generated. For instance, if the total momentum  $P = p_1 - p_2$  of the vertex vanishes, the vertex  $\Gamma_A$  is simply identical to  $2B(p)\gamma_5$ , where  $B(p)$  is a finite solution of the mass gap equation. This vertex describes the coupling of the pion to two quarks, and eqn. (6) shows that in the chiral limit we have a Goldstone boson, the pion.

For simplicity the flavor is not yet included. Flavor will only be explicitly included at the end of subsection VII. The isoscalar axial Ward identity must include the Axial anomaly, which is crucial to the  $U(1)$  problem. Nevertheless the pion is an isovector, and in the coupling of a pion we do not need to concern with the Axial anomaly.

We now derive a powerful Ward identity for the ladder which involve the axial vertices and the ladder. This relation is depicted in Fig. 5, it constitutes an extension of the Ward Identity for the propagators in eqs. (7) and (8). This identity is derived if we expand [10, 20, 21] the ladders and substitute the vertex in the left hand side. Then all terms with an intermediate  $\gamma_5$  include the anticommutator  $\{\gamma_5, \gamma_\nu\}$  and this cancels because *the interaction is chiral invariant and the kernel is local*. Only the right hand side survives.

We are now ready to derive the mass gap and the boundstate equations beyond rainbow-ladder truncation, to include the diagrams that are able to generate  $\eta$ - $\eta'$  mass difference. Starting from the diagram in Fig. 3 (a) (which is the minimal diagram that involves one  $t$ -channel meson exchange), and substituting the Bethe-Salpeter vertex by a propagator, we arrive at the contribution for the quark self-energy in Fig. 6. Notice that,

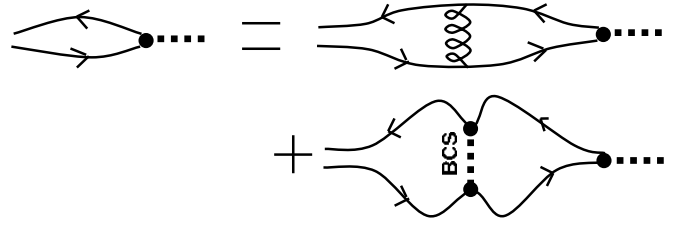


FIG. 10: The homogeneous Bethe-Salpeter equation we solve here. The kernel includes the BCS level One Gluon Exchange, the anomalous annihilation into two gluons, and the non-perturbative One Pion Exchange.

to remove any disconnected diagrams, the first diagram must include at least one gluon exchange, thus, in Fig. 6, the geometric series starts with one gluon exchange.

Then, inserting the Bethe-Salpeter vertex in all possible propagators of the quark self-energy, we get the kernel diagrams in Fig. 7 for the boundstate equations. The first kernel diagram is obtained inserting the vertex in the only propagator of the self-energy exterior to the ladder. The second kernel diagram is obtained inserting the vertex in the same quark line, but inside the ladder of the self-energy. The third kernel diagram is obtained inserting the vertex in the quark line linking to the external legs of the self-energy. We can also express these diagrams in terms of ladders only, and we finally get the diagrams in Figs. 8 and 9. In Fig. 8 we show the diagrams contributing to the  $U(1)_A$  mass splitting and in Fig. 9 we show the diagrams contributing to all mesons.

### III. A CALCULABLE BETHE SALPETER KERNEL

We now choose the best framework to compute the new beyond BCS diagrams. Notice that the diagrams in Figs. 6, 8 and 9 all include full ladders, and an integral in one of the relative variables of the full ladder. Technically this remains a problem since it goes beyond the present state of the art of quark models.

Two different classes of quark models, consistent with chiral symmetry, have been investigated and applied to different problems. The equal time quark models are confining, thus they are adequate for the computation of the full ladder, including the full spectrum of mesons. However they are not Lorentz invariant and thus are inadequate for the boost of the ladder, occurring in the momentum space integral in the Feynman diagrams. And the Lorentz non-invariance also splits the time-like from the space-like components and observables of the model. On the other hand, the euclidian space quark models are convenient for full integrations of internal momenta in Feynman diagrams, but are not confining and thus are inadequate for the computation of the full ladder. However, the full ladders can be replaced by the lowest boundstate contribution, i. e. approximately assumed to

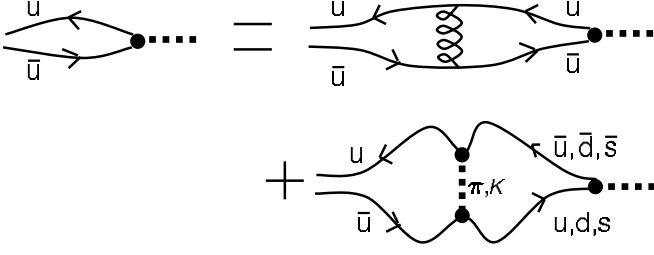


FIG. 11: An example of BSE equation needed to solve for the mass of the bound state  $u\bar{u}$ . In the annihilation diagram quark propagators of all flavors contribute. That makes it necessary to include kaon exchange in this diagram if the strange flavor is taken into account.

be similar to the pseudoscalar pole contribution. In this case the euclidian models, essentially adequate to address the lowest energy phenomena of hadronic physics (including the pseudoscalar ground states to the vector ground states and pseudoscalar first excitations), can be applied to the  $U(1)_A$  breaking of the pseudoscalar spectrum.

The dominant part of the non-perturbative dressing of the kernel of the Bethe Salpeter equation with hadron ladders is the One Meson Exchange in the t-channel. Notice that the corresponding diagram occurs with two minus signs when compared with the One Gluon Exchange. A first minus sign is necessary to cancel all the disconnected diagrams. A second minus sign is due to the fermion loop.

Now, t-channel exchange is dominated by the pseudoscalar meson exchange, since the pseudoscalar mesons are the lightest ones. Thus, in this first attempt of the  $\eta'$  mass study beyond BCS, we will approximately saturate the meson exchange with only the ground state pseudoscalar nonet. And, because we are mostly interested in the  $U(1)_A$  breaking, we will also neglect all terms that contribute equally to all mesons, providing only a constant overall mass shift of the different spectra. Thus we will not consider the contribution to the mass gap equation of Fig. 6 and the contribution to the mass gap equation of Fig. 9 (it has also been estimated by one of us [10] that these effects are relatively small). In any case, these two effects cancel in the chiral limit, since our self-consistent approach complies with the Goldstone theorem.

The minimal kernel necessary to estimate the different contributions to the  $\eta$  and  $\eta'$  masses is presented in Fig. 10. The first diagram on the right-hand-side of Fig. 10 is the BCS level One Gluon Exchange. This diagram contributes to all mesons. The second diagram on the right-hand-side includes the pion exchange in t-channel between quark and antiquark. It only contributes to the isosinglet mesons, and therefore generates the mass difference between the  $\pi_0$ , the  $\eta$  and the  $\eta'$ .

The diagrammatic form of Bethe-Salpeter equation depicted in Fig. 10 can be written as,

$$\Gamma_\eta^{aa}(p; P) = \quad (12)$$

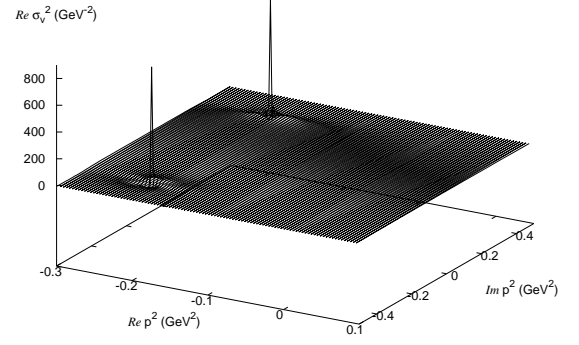


FIG. 12: Singularities of the solution of the gap equation for  $u$  quark. The real part of the scalar function  $\sigma_v(p^2)$  is presented, which is defined in (16).

$$\begin{aligned} & \int \frac{d^4 q}{(2\pi)^4} K(p, q; P) S^a(q + \eta P) \Gamma_\eta^{aa}(q; P) S^a(q - \beta P) \\ & + \sum_{M,b} \int \frac{d^4 q}{(2\pi)^4} C_M^{ab}(p, q; P) S^b(q + \eta P) \Gamma_\eta^{aa}(q; P) S^b(q - \beta P), \end{aligned}$$

where

$$C_M^{ab}(p, q; P) = \Gamma_M^{ab}(p, q, P) G_M(p - q) \Gamma_M^{ba}(p, q, P), \quad (13)$$

$\Gamma_M^{ab}$  is the Bethe-Salpeter amplitude and  $G_M$  is the propagator of the meson being exchanged,  $a$  and  $b$  denote quark flavors.

The effective running coupling in the kernel can be modeled to account for the effects of the truncation. We used the Maris-Tandy model [22, 23] in our calculations,

$$\frac{G(k^2)}{k^2} = \frac{4\pi^2 D}{w^6} k^2 e^{-k^2/w^2} + \quad (14)$$

$$\frac{4\pi^2 \gamma_m F(k^2)}{\frac{1}{2} \ln \left[ \tau + \left( 1 + k^2/\Lambda_{QCD}^2 \right)^2 \right]}, \quad (15)$$

where  $F(k^2) = \left( 1 - \exp \frac{-k^2}{4m_t^2} \right) / k^2$ ,  $\gamma_m = 12/(33 - 2N_f)$  and where the parameters are  $m_t = 0.5$  GeV,  $N_f = 4$ ,  $\Lambda_{QCD} = 0.234$  GeV,  $\tau = e^2 - 1$ ,  $D = 0.93$  GeV<sup>2</sup> and  $w = 0.4$  GeV. This model has been shown to work well for the description of the light meson properties (see for example [24, 25]). Therefore we expect it to give sensible results for the masses of  $\eta$  and  $\eta'$ .

In general, for  $N_f$  quark flavors there will be  $N_f$  coupled integral Bethe-Salpeter equations, which have to be solved together. An example of such an equation for the  $u\bar{u}$  bound state with all possible pseudoscalar meson exchanges is depicted in Fig. 11.

Notice that one of the features of Schwinger-Dyson equation approach is the fact that the solution for the quark propagator has singularities. An example of the

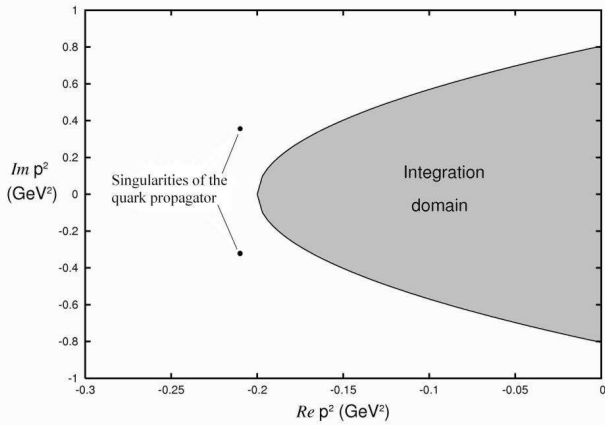


FIG. 13: Location of the singularities of the quark propagator with respect to our largest integration domain of Bethe-Salpeter equations.

solution for the function  $\sigma_v(p^2)$  for the  $u$  quark,

$$\sigma_v(p^2) = \frac{A(p^2)}{p^2 A^2(p^2) + B^2(p^2)}. \quad (16)$$

is presented in Fig. 12. In general, these singularities can pose a serious technical problem for the numerical calculations if present in the integration domain of the integral Bethe-Salpeter equations. However, we have checked that in our case these singularities are outside from the largest integration domain that we have. Our largest integration domain and the positions of the poles are shown in Fig. 13.

Thus the masses of the  $\eta$  and  $\eta'$  mesons are computable in the SDE and BSE formalism, extending the Klabucar and Kekez parametrization of the  $U_A(1)$  breaking [27].

#### IV. RESULTS

We solve the Bethe-Salpeter equation (12) for the pseudoscalar mesons. This equation takes into account the additional “annihilation” diagram which contributes to the isoscalar but not to the isovector mesons.

This additional diagram is depicted in Fig. 3a, it consists of the annihilation of our  $q\bar{q}$  pair into an infinite gluon ladder. If calculated perturbatively, this diagram does not contribute to the isoscalar meson mass in the chiral limit. However, it gives rise to the  $\eta'$  meson mass if treated nonperturbatively. We propose to represent the infinite gluon ladder in the “annihilation” diagram as a t-channel meson exchange. In general, mesons in a t-channel can have any quantum numbers. However, the pion and the other members of the pseudoscalar octet, being the lightest mesons, give the dominant contribution.

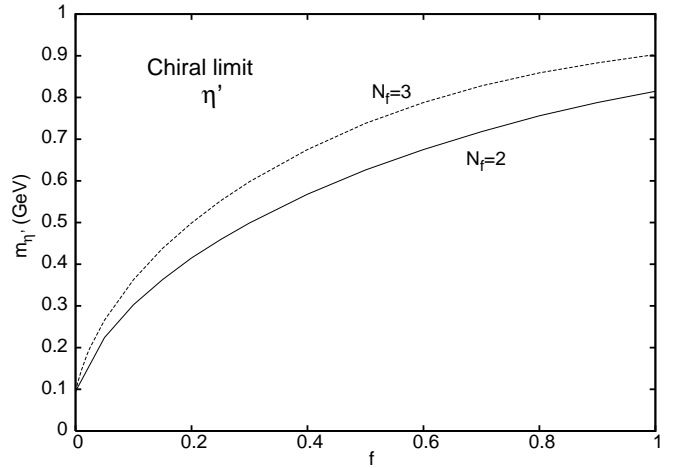


FIG. 14: Dependence of the mass of  $\eta'$  meson on the “weight” of the additional diagram in the chiral limit for two and three quark flavors.

This  $U_A(1)$  breaking term is added to the ladder Bethe-Salpeter kernel in the Bethe-Salpeter equation (12), as in Fig. 10. The Bethe-Salpeter amplitude, needed for the pseudoscalar-exchange kernel, is previously calculated by solving Bethe-Salpeter equation in the ladder truncation (9). The quark propagator, which is needed for the solution of the equation (12) is also obtained by solving the ladder Schwinger-Dyson equation (1) numerically. This ensures that the pion and kaon non-isoscalar masses are unaffected. Having thus defined both the Bethe-Salpeter kernel and the quark propagator, we solve numerically the Bethe-Salpeter equation by the power method.

First, we investigate the isoscalar meson mass in the chiral limit. The chiral limit is the limit where the current quark masses vanish. In this case the “annihilation” diagram is simply proportional to the number of flavors  $N_f$ . From the extent of the  $U_A(1)$  breaking it is expected, that when the chiral limit is taken for all three quark flavors, the  $\pi_0$  and  $\eta$  should become massless, and the  $\eta'$  should remain massive. We are able to reproduce this behavior with our phenomenological model: the “annihilation” diagram does not contribute to the  $\pi_0$  and  $\eta$  in the chiral limit leaving these mesons massless, but changes the mass of the flavor scalar  $\eta'$  (Fig. 14).

The Bethe Salpeter amplitude of pseudoscalar mesons can be decomposed into four Dirac structures  $E, F, G, H$ . By keeping only the  $E$  amplitude (separable in the chiral limit and dominant for realistic masses) we calculate the  $\eta'$  meson mass in the chiral limit with the dependence on the “weight” of the additional diagram (phenomenological factor  $f$  which multiplies the additional  $U_A(1)$  breaking diagram in the BSE). The result for 2 and 3 quark flavors is presented in Fig. 14. In the two-flavor case there is only one  $\eta$ , in Fig. 14 it is also denoted  $\eta'$ . One can see that our calculations give a very reasonable estimate of the mass of  $\eta'$  in the chiral limit. The solutions of the Bethe-Salpeter equation for  $\pi, K$  and  $\eta'$  (in the chiral limit) are presented in Fig.

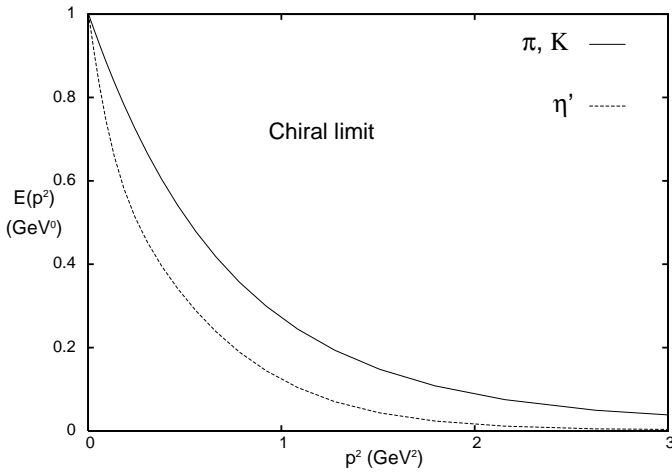


FIG. 15: The  $E(p^2)$  Bethe-Salpeter amplitudes, solutions of Bethe-Salpeter equation, for the  $\pi$ , the  $K$  and the  $\eta'$ .

15. Notice that in the chiral limit the pion and kaon amplitudes are identical.

Next, in our calculation, we employ broken  $SU(3)_f$  symmetry with  $u$  and  $d$  quarks of equal finite mass, and realistically heavier  $s$  quark. That means that in the "annihilation" diagram we have to include both kaon and pion propagators. We examine the effect that this diagram has on the physical mesons. It has been shown before [24] that the SDE and BSE approach, in the rainbow-ladder truncation, works reasonably well for the properties of the light isovector mesons, and we reproduce these results obtaining for the pion  $m_\pi = 0.139$  GeV and  $f_\pi = 0.131$  GeV.

The  $SU(3)_f$  octet and singlet isospin zero states,  $\eta_8$  and  $\eta_0$ , can be expressed in the  $q\bar{q}$ -basis,

$$|\eta_8\rangle = \frac{1}{\sqrt{6}} (|u\bar{u}\rangle + |d\bar{d}\rangle - 2|s\bar{s}\rangle), \quad (17)$$

$$|\eta_0\rangle = \frac{1}{\sqrt{3}} (|u\bar{u}\rangle + |d\bar{d}\rangle + |s\bar{s}\rangle). \quad (18)$$

while in  $SU(2)_f$  only the  $\eta_0$  state is defined. The "annihilation diagram" does not contribute to the mass of  $\eta_8$  in the chiral limit. For the finite quark masses, however, it does still contribute due to the mass difference of  $u(d)$  and  $s$  quarks. For  $\eta_0$  this diagram makes a difference both in chiral limit and in the finite quark mass case. To find the masses of the  $\eta_0$  and  $\eta_8$  we have to solve the system of two coupled integral BSEs (one for  $u(d)$  and one for  $s$  flavor), equivalent to the equation (12). An example of such an equation for the  $u\bar{u}$  channel, including its coupling to the  $d\bar{d}$  and  $s\bar{s}$  channels, is depicted diagrammatically in Fig. 11. The dependencies of  $\eta_0$  and  $\eta_8$  meson masses on the "weight" factor  $f$  are presented in Fig. 16 and 17. The full BSE has been solved for each "weight" factor.

To make a connection with the physical mass eigenstates, we introduce the mixing angle  $\Theta$ ,

$$|\eta\rangle = \cos\theta|\eta_8\rangle - \sin\theta|\eta_0\rangle, \quad (19)$$

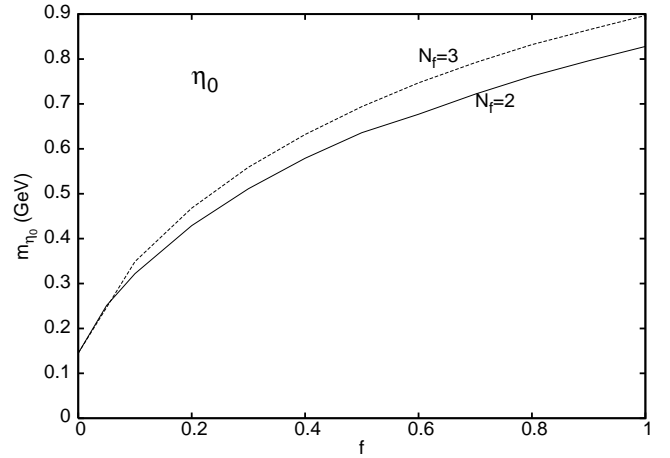


FIG. 16: Dependence of the flavor scalar  $\eta_0$  mass on the "weight" factor  $f$  for two and three quark flavors.

$$|\eta'\rangle = \sin\theta|\eta_8\rangle + \cos\theta|\eta_0\rangle. \quad (20)$$

By comparing the results of our calculation to the experimental values of  $\eta$  and  $\eta'$  mass we can determine the mixing angle  $\theta$ ,

$$\tan^2\Theta = \frac{M_{\eta_8} - M_\eta}{M_{\eta'} - M_{\eta_8}} \quad (21)$$

$$\tan^2\Theta = \frac{M_{\eta'} - M_{\eta_0}}{M_{\eta_0} - M_\eta}. \quad (22)$$

For the "weight" factor  $f = 0.9$  we obtain  $\Theta \approx -28^\circ$  in reasonable agreement with experiment, which favors the mixing angle in the vicinity of  $-20^\circ$  [27, 28]. Now we can use this angle to explore the dependence of the physical  $\eta$  and  $\eta'$  on the weight factor. The corresponding results are presented in Fig.18.

## V. CONCLUSION

We identify a full one-quark-loop class of microscopic quark diagrams contributing to the  $\eta$  and  $\eta'$  masses, separating these pseudoscalar mesons from the  $\pi$  and  $K$  mesons.

Because it is not yet possible to compute the full class of diagrams, we identify the dominant diagrams, equivalent to the exchange of the ground state pseudoscalar mesons.

Nevertheless this problem still requires state of the art techniques. We avoid the equal-time framework, where the number of diagrams would be much larger because the quark propagators would be separated from the antiquark propagators. We adopt the Euclidian time Schwinger Dyson framework. The Bethe-Salpeter equation turns out to be solvable, because the poles in the solution of the gap equation, for negative Euclidian momentum, does not cross the complex domain of integration in the Argand plot of the momentum, depicted in



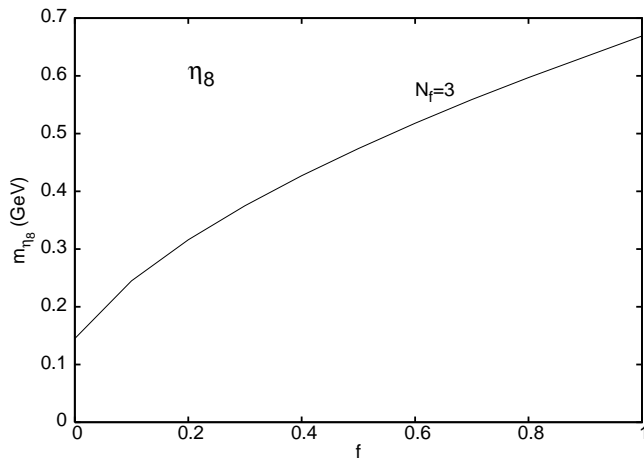


FIG. 17: Dependence of the  $\eta_8$  mass on the "weight" factor  $f$  for three quark flavors.

Fig. 13. Together with the isovector ground state pseudoscalars [23, 24, 25], first excited pseudoscalar states [26] and ground state vectors [22], this is a new case among the few where the Euclidian Bethe Salpeter equation has been solved so far.

We notice that the infrared part of the complete class of diagrams should vanish in the chiral limit. Only the ultraviolet anomaly of Adler Bell and Jackiw should survive in that limit. Thus it is a priori expected that our dominant diagram should be excessive to produce the  $\eta$  and  $\eta'$  masses, since a cancelation with the other diagrams should occur in the chiral limit. Hence we multiply this diagram by a reducing factor  $f$ . We find that our diagram is indeed dominant since only the factor  $f = 0.9$  is necessary to arrive at the correct experimental masses. Importantly, we then essentially comply with the experimental mixing of the  $\eta_0$  and  $\eta_8$ .

Our results show that the quark model may solve the U(1) problem with simple microscopic interactions, although new technical advances in the computation of full ladders are necessary before this problem is fully solved. More progresses may be achieved with the computation of contributions to the diagrams in Fig. 3 (b) and with the separation of the infrared and of the ultraviolet contributions to the  $\eta$  and  $\eta'$  masses.

Importantly we also study the case where there are only two light flavors. This case is not realistic, nevertheless it is important to be compared with the two-flavor studied in Lattice QCD. In this two-flavor case we find that the  $\eta'$  mass is only reduced by 20%. This stresses the relevance of two-flavor studies in Lattice QCD.

On the other hand, the importance of the one-pion exchange diagram explains why Lattice QCD, with the present size of the lattices, cannot directly reproduce the  $\eta$  and  $\eta'$  masses. Since the pion is very light, a large lattice will be necessary to encompass with no chiral extrapolation the extent of the one pion exchange potential between the quarks.

#### Acknowledgments

PB thanks discussions on the relevance of glueballs with Felipe Llanes-Estrada. OL would like to thank Peter Tandy, Nicholas Souchlas, Reinhard Alkofer and Andreas Krassnigg for useful conversations. PB was supported by the FCT grants POCI/FP/63437/2005 and POCI/FP/63405/2005. OL was supported in part by the U.S. National Science Foundation under Grant Nos. PHY-0610129.

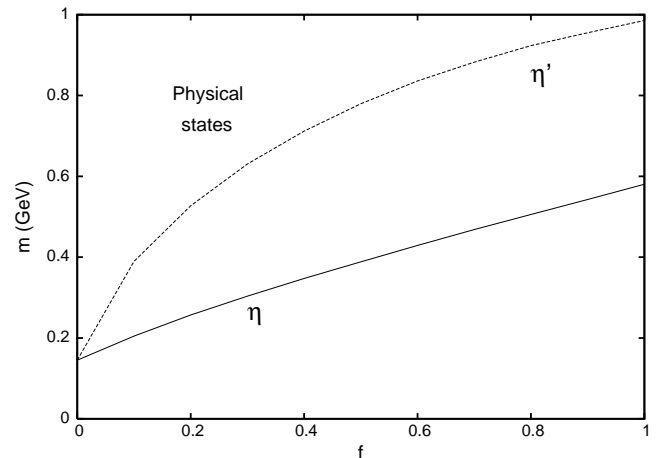


FIG. 18: Dependence of the physical state masses  $\eta$  and  $\eta'$  on the "weight" factor  $f$ .

- 
- [1] S. Weinberg, Phys. Rev. D **11**, 3583 (1975).
  - [2] Y. Nambu and G. Jona-Lasinio, Phys. Rev. **124** (1961) 246.
  - [3] M. Gell-Mann and M. Levy, Nuovo Cim. **16**, 705 (1960).
  - [4] G. 't Hooft, Phys. Rev. D **14**, 3432 (1976) [Erratum-ibid. D **18**, 2199 (1978)].
  - [5] A. A. Osipov, B. Hiller and J. da Providencia, Phys. Lett. B **634**, 48 (2006) [arXiv:hep-ph/0508058].
  - [6] A. Duncan, E. Eichten, S. Perrucci and H. Thacker, Nucl. Phys. Proc. Suppl. **53**, 256 (1997) [arXiv:hep-lat/9608110].
  - [7] Y. Kuramashi, M. Fukugita, H. Mino, M. Okawa and A. Ukawa, Phys. Rev. Lett. **72**, 3448 (1994).
  - [8] E. Witten, Nucl. Phys. B **156**, 269 (1979).
  - [9] S. Aoki *et al.* [JLQCD Collaborations], PoS **LAT2006**, 204 (2006) [arXiv:hep-lat/0610021].
  - [10] P. J. A. Bicudo, Phys. Rev. C **60**, 035209 (1999) [arXiv:nucl-th/9802058].
  - [11] C. S. Fischer, D. Nickel and J. Wambach, arXiv:0705.4407 [hep-ph].
  - [12] S. L. Adler, Phys. Rev. **177**, 2426 (1969).
  - [13] S. L. Adler and W. A. Bardeen, Phys. Rev. **182**, 1517

- (1969).
- [14] J. S. Bell and R. Jackiw, *Nuovo Cim. A* **60**, 47 (1969).
  - [15] G. 't Hooft, *Phys. Rev. Lett.* **37**, 8 (1976).
  - [16] L. von Smekal, A. Mecke and R. Alkofer, *arXiv:hep-ph/9707210*.
  - [17] L. von Smekal, R. Alkofer and A. Hauck, *Phys. Rev. Lett.* **79**, 3591 (1997) [*arXiv:hep-ph/9705242*].
  - [18] P. Maris and C. D. Roberts, *Int. J. Mod. Phys. E* **12**, 297 (2003) [*arXiv:nucl-th/0301049*].
  - [19] A. Holl, C. D. Roberts and S. V. Wright, *arXiv:nucl-th/0601071*.
  - [20] P. Bicudo, *Phys. Rev. C* **67**, 035201 (2003) [*arXiv:hep-ph/0311277*].
  - [21] F. J. Llanes-Estrada and P. De A. Bicudo, *Phys. Rev. D* **68**, 094014 (2003) [*arXiv:hep-ph/0306146*].
  - [22] P. Maris and P. C. Tandy, *Phys. Rev. C* **60**, 055214 (1999) [*arXiv:nucl-th/9905056*].
  - [23] P. Maris and C. D. Roberts, *Phys. Rev. C* **56**, 3369 (1997) [*arXiv:nucl-th/9708029*].
  - [24] P. Maris, C. D. Roberts and P. C. Tandy, *Phys. Lett. B* **420**, 267 (1998) [*arXiv:nucl-th/9707003*].
  - [25] P. Maris and P. C. Tandy, *Phys. Rev. C* **62**, 055204 (2000) [*arXiv:nucl-th/0005015*].
  - [26] A. Holl, A. Krassnigg and C. D. Roberts, *Phys. Rev. C* **70**, 042203 (2004) [*arXiv:nucl-th/0406030*].
  - [27] D. Klabucar and D. Kekez, *Phys. Rev. D* **58**, 096003 (1998) [*arXiv:hep-ph/9710206*].
  - [28] W. M. Yao *et al.* [Particle Data Group], *J. Phys. G* **33**, 1 (2006).